Effects of aspen harvesting on groundwater recharge and water table dynamics in a subhumid climate

J. J. Carrera-Hernández,[1,2] C. A. Mendoza,[1] K. J. Devito,[3] R. M. Petrone,[4] and B. D. Smerdon[5]

Received 21 June 2010; revised 18 January 2011; accepted 8 February 2011; published 28 May 2011.

[1] Numerical experiments were developed using different water table depths and soil textures to investigate the impact of aspen harvesting on hydrological processes on the Western Boreal Plain. The effect of harvesting on soil moisture dynamics, fluxes at the water table, and water table fluctuation were compared for different harvesting scenarios simulated under wet and dry climatic cycles. Strong interaction between shallow water tables (i.e., 2 m) and atmospheric variability is observed for all soil textures and is reduced as the vadose zone thickens, particularly after a dry cycle, as a series of positive net atmospheric fluxes are needed to reduce soil moisture storage in order for recharge to occur. Because of harvesting, the water table fluxes can increase by 50 mm month^{-1}, while on a yearly basis, this increase can reach 200 mm yr^{-1}, with rainfall events taking between 1 and 5 years to become recharge (i.e., time lag). Also, the water table is expected to rise between 1 and 3.5 m, with rainfall–water table rise time lags of 1–3 years; however, the peak manifestation of harvesting on water table elevation can take up to 7 years after harvesting. The effects of aspen harvesting are more pronounced during wet cycles, and the development of forestry activities in the Boreal Plain should consider not only preceding precipitation but also the preceding precipitation–reference evapotranspiration ratio, water table depth, and soil texture. The interaction of these factors needs to be considered in order to develop sustainable forestry plans and avoid waterlogging conditions.

Citation: Carrera-Hernández, J. J., C. A. Mendoza, K. J. Devito, R. M. Petrone, and B. D. Smerdon (2011), Effects of aspen harvesting on groundwater recharge and water table dynamics in a subhumid climate, *Water Resour. Res., 47*, W05542, doi:10.1029/2010WR009684.

1. Introduction

[2] Forest harvesting affects the hydrological cycle because interception, infiltration, and evapotranspiration are modified; according to *Roy et al.* [1997], the major change following clear-cutting is water table rise, referred to as "watering-up," which can decrease site productivity by delaying forest regeneration and reducing tree growth [*Dubé and Plamondon*, 1995]. Depending on water table depth, this effect may decrease the depth of the aerated zone for tree root exploitation [*Landhäusser et al.*, 2003] and should be avoided in order to adequately manage forestry activities. *Bosch and Hewlett* [1982] presented a summary and review of 94 catchment experiments comprising different vegetation types (such as eucalypts, deciduous hardwood, and scrub), concluding that water yield response (i.e., runoff) to harvesting depends on both the mean annual precipitation and the precipitation for the harvesting year. According to them, changes in water yield are more persistent in drier areas because of the slow recovery of vegetation but are related to precipitation during the year of treatment. This statement is reinforced by the observations of *Peck and Williamson* [1987] and *Ruprecht and Schofield* [1991], who found that water table response to eucalypt removal depended on precipitation and water table depth. They report the observations of a long-term study that took place in southwest Western Australia, where in the early 1970s, five experimental catchments were established within the Collie Basin. The effect of forest clearing on the water table was a function of its depth and rainfall: when it was found about 3.5 m below surface before clearing, the water table intersected the surface after 3 years [*Peck and Williamson*, 1987]. *Ruprecht and Schofield* [1991] found that the effect of clearing on the water table is not immediate: on the low-rainfall catchments, where the water table was 30 m deep, the average rise rate was 0.11 m yr^{-1} in the first 4 years (1977–1980), increasing to 1.45 m yr^{-1} during 1981–1985 and 2.3 m yr^{-1} in 1986–1989, with a maximum rate of 4.8 m yr^{-1}. The total water table rise in 13 years was 15 m in the valley and 20 m on the lower side slopes. In these catchments, the existing eucalypt forest was cleared for agriculture.

[3] The effect of forest harvesting of different species has been studied in many geographic and climatic regions,

[1]Department of Earth and Atmospheric Sciences, University of Alberta, Edmonton, Alberta, Canada.
[2]Now at Instituto Potosino de Investigación Científica y Tecnológica, San Luis Potosí, México.
[3]Department of Biological Sciences, University of Alberta, Edmonton, Alberta, Canada.
[4]Department of Geography and Environmental Studies, Wilfrid Laurier University, Waterloo, Ontario, Canada.
[5]CSIRO Land and Water, Glen Osmond, South Australia, Australia.

0043-1397/11/2010WR009684

most often with a focus on changes to catchment water yield. This has been the focus of aspen harvesting studies by *Verry* [1987] in Minnesota and by *Swanson and Rothwell* [2001] for the Keg River Basin in northwestern Alberta. In the Pacific Northwest (see review by *Moore and Wondzell* [2005]), hydrological recovery typically occurs within 10–20 years in coastal catchments but may take many decades in mountainous, snow-dominated catchments with varying tree species (mainly conifers). In humid regions of the Canadian Boreal Shield, timber harvesting (coniferous and deciduous) results in increased base and peak flows because of decreased snow and rainfall interception and increased infiltration [*Buttle et al.*, 2000]. In eastern Canada, *Marcotte et al.* [2008] found that 10 years after clear-cutting mixed wood stands (dominated by balsam fir, eastern white cedar, and red maple), water table elevations were still 5–7 cm higher than precut levels, with slow water table recovery after the third year. During the first growing season after cutting, *Pothier et al.* [2003] found that the water table rise was linearly related to the percentage of area cut in a conifer stand and that 5 years after cutting, the water table was gradually approaching the precutting levels; however, the water table was still higher. A water table rise was also reported by *Dubé and Plamondon* [1995] after clear-cutting mixed wood stands (eastern white cedar, red maple, red spruce, balsam fir, and yellow birch) on wetlands of the St. Lawrence lowlands. On the Boreal Plain, *Whitson et al.* [2005] found a trend toward greater soil moisture for 3 years after harvest, despite dry weather and rapid reestablishment of aspen, while *Devito et al.* [2005] determined the water balance and runoff regime of an aspen-forested catchment on the Boreal Plain for 5 years after a partial timber harvest. They found that in most years the water balance was dominated by soil water storage, evapotranspiration, and vertical recharge. While each of the studies undertaken in various geographic regions focuses on different aspects controlling overall catchment water yield, few explicitly investigate the direct linkages between harvest, changes in water table dynamics, and groundwater recharge.

[4] To understand the controls on recharge and the effect of aspen harvesting on the Boreal Plain, this work uses a physically based numerical model to simulate harvesting scenarios. The advantage of physically based models is that they can be used to identify and quantify linkages between forest management activities and affected resources by considering the various controlling processes such as rainfall, interception, snowmelt, and evapotranspiration [*Alila and Beckers*, 2001]. The effect of aspen harvesting in the Boreal Plain is addressed, as this species is the most important deciduous tree in the Canadian Boreal Plain, both ecologically and commercially [*Hogg et al.*, 2002], yet harvesting effects have only been investigated through water yield studies [*Swanson and Rothwell*, 2001]. On the subhumid Boreal Plain, the spatial and temporal variability of soil water storage capacity in relation to evaporation and precipitation deficits complicates interpretation of forest harvesting studies, and low runoff responses may mask the overall impacts of aspen harvesting in headwater areas [*Devito et al.*, 2005]. Thus, the water stored in the soils of boreal forest stands reflects complex interactions between soil, canopy, and vegetation water use characteristics [*Elliott et al.*, 1998], where the potential to exceed upland soil water storage capacity and to generate significant runoff may only occur about once every 25 years [*Redding and Devito*, 2008].

2. Methodology

[5] Numerical experiments were developed using different water table depths and soil textures in order to understand the impact of aspen harvesting. Daily climatological data from Fort McMurray (1919–2006) were used as input into the model, along with measured reference and actual evapotranspiration rates (ET_0 and ET, respectively) on aspen stands. On much of the Boreal Plain (Figure 1), both the subhumid climate ($P \leq ET_0$) and the deep glacial sediments result in large available soil storage capacity [*Redding and Devito*, 2008]; accordingly, it is expected that unsaturated zone storage and vertical flow will dominate, rather than lateral flow or runoff [*Devito et al.*, 2005]. This interaction of hydrological processes was quantified by *Redding and Devito* [2008], who found that runoff occurrence in this region has a return period of 25 years or more. In addition, where there is potential for diffuse recharge, the movement of moisture through the vadose zone is usually a one-dimensional process [*Stephens*, 1993]. The combination of climatic and geologic characteristics of the Boreal Plain is unique in the Canadian Boreal Forest, compared to adjacent Boreal Shield and Cordillera regions, and was the impetus for the Hydrology, Ecology and Disturbance (HEAD) project in northern Alberta [*Smerdon et al.*, 2005], which developed a series of hydrologic studies at the Utikuma Region Study Area (URSA, Figure 1), located approximately 60 km southwest of Fort McMurray. This work builds on previously undertaken research at URSA in both fine-textured soil (URSA study sites 43 and 171, Figure 1 [*Ferone and Devito*, 2004]) and outwash deposits (URSA study site 16, Figure 1 [*Smerdon et al.*, 2005, 2008, 2007]) and water table depths measured at different URSA sites (Figure 1).

[6] To understand groundwater recharge dynamics and the effect of harvesting on fluxes at the water table (i.e., recharge and upward flux) in this region, transient moisture flow in the vadose zone must be explicitly considered. Consequently, a number of numerical experiments were executed to estimate recharge fluxes and soil moisture dynamics on undisturbed aspen sites for the entire period (1919–2006). Subsequent harvesting scenarios were simulated using end-members of climatological conditions.

[7] The simulations were run using the numerical code HydroGeoSphere (HGS) [*Therrien et al.*, 2010], which uses the control volume finite element method to solve the flow equations for all domains considered in a simulation. HGS solves either linear equations (for fully saturated flow or solute transport) or nonlinear equations (for variably saturated subsurface flow and surface flow). To solve the nonlinear equations, HGS uses the Newton-Raphson linearization method and a preconditioned iterative solver for the matrix equation. Although HGS can be used to simulate interception and evapotranspiration through the use of the leaf area index (LAI) and a time-varying root distribution function [*Kristensen and Jensen*, 1975], it still requires three dimensionless fitting parameters, for which available data did not suffice. To reduce uncertainty in the developed model, the field measurements of both ET_0 and ET were used to derive a relationship that was considered to be constant during the

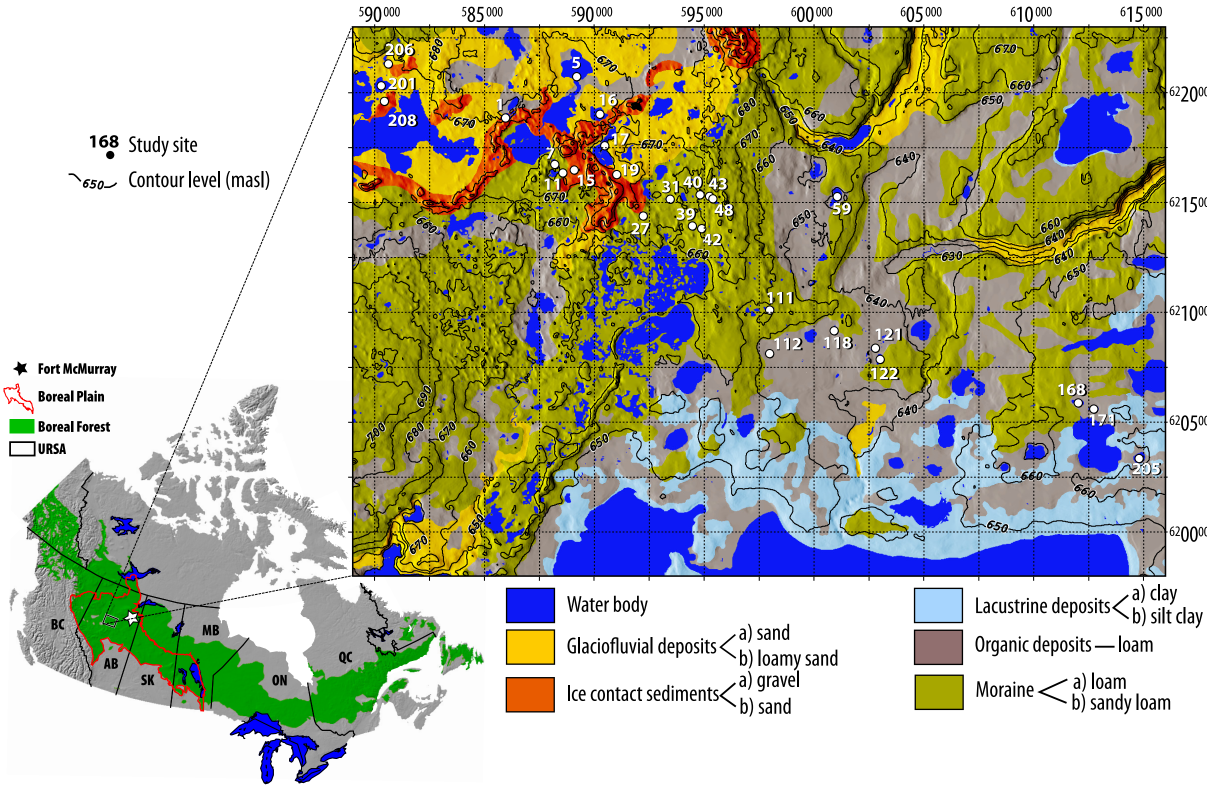

Figure 1. Surficial geology of the Utikuma Region Study Area (URSA), located within the Boreal Plain. Also shown are the study sites located within this region. The textures used on the numerical models of this work were selected on the basis of URSA's surficial geology, as indicated in the legend. On the transition areas the texture changes (i.e., the moraine changes from loam to sandy loam toward both the glaciofluvial deposits and ice contact sediments). The short-term ET_0 and ET data used in this work were measured on sites 40 and 43 of URSA, while long-term data from Fort McMurray were used.

long-term simulation, as described in section 2.1. Readers interested in the details of HGS are encouraged to read its comprehensive documentation [*Therrien et al.*, 2010].

2.1. Atmospheric Fluxes

[8] The numerical experiments required that net atmospheric fluxes be applied to the top of soil columns. Such fluxes were determined by subtracting daily actual evapotranspiration from precipitation, including snow water equivalent. The details of this implementation follow.

2.1.1. Evapotranspiration

[9] Long-term climatological data from Fort McMurray do not include daily ET_0. Thus, daily ET_0 (mm d^{-1}) had to be derived from daily climatological data available from the Fort McMurray climate station. Although the Penman-Monteith method is generally recommended [*Allen*, 2000], data at this location were not available for its application; thus, the *Hamon* [1963] method was selected in this work. This method has been used by a large number of authors, including recent studies in the Willow River watershed [*Clark et al.*, 2009] and in the Utikuma drainage basin [*Sass and Creed*, 2008], both of which are also located within the Boreal Plain ecozone. The Hamon method relates the reference evapotranspiration (ET_0) with air temperature:

$$ET_0 = 29.8D\frac{e_a^*}{T_a + 273.2}, \tag{1}$$

where e_a^* is the saturation vapor pressure (kPa) at the mean daily temperature T_a (°C) and D is day length (hours). Evapotranspiration data (ET and ET_0) were collected using the eddy covariance technique [*Baldocchi et al.*, 1988] at two locations within the URSA. Turbulent flux data, radiation, and energy flux information were also collected at the tower locations during the same periods. Flux and energy data were collected from the aspen-dominated uplands in the study catchment on both north facing and south facing slopes (NFS and SFS, respectively). Because this study catchment was harvested during the study period (SFS in the winter of 2007; NFS in the winter of 2008), data collected from the two upland areas during the 2005–2008 period include both mature aspen stands (66 years) and 1- and 2-year-old regenerated aspen stands. Although actual start and end dates of the measurement campaign at the URSA site varied slightly between years, on average, flux measurements spanned early May to late September (with the exception of 2005, when initial installation of the first tower did not occur until late June).

[10] From these field measurements, a ratio between ET_0 and ET (α) was determined for mature and early chronosequence regenerating aspen (Figure 2), through the use of data from other representative aspen stands in northern Saskatchewan and Alberta [*Grant et al.*, 2009; *Blanken et al.*, 1997, 1998, 2001; *Amiro et al.*, 2006]; these data are summarized in Table 1. The α values thus determined for a

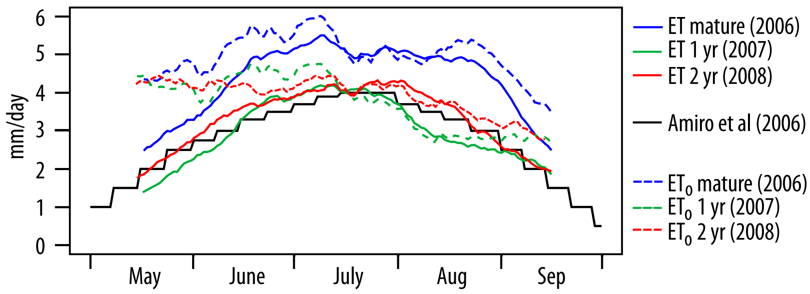

Figure 2. The 30 day moving average for ET_0 and ET measured at mature and regenerating aspen stands. This moving average was selected to smooth out the variability of daily data. The ET values of *Amiro et al.* [2006] measured at the Old Aspen site in central Saskatchewan are shown for comparison.

range of stand ages were then applied to the long-term ET_0 values obtained through equation (1) to develop the 1919–2006 daily ET values used in the simulations. The α ratio varies within a year (Figure 2), with lower values in May and peak values in July; this ratio was assumed constant for all years. While the stand ET recovers quickly, this does not necessarily mean the partitioning of the flux among the aspen and other competing emerging species is "natural;" however, in terms of the net vertical water loss from the system, predisturbance levels have been achieved [*Amiro et al.*, 2006]. Although it would be expected for the α ratio to exhibit some interannual variability over the considered period, the uncertainty introduced by its uniformity is also expected to be minimal because it is well documented that the relationship between ET_0 and ET is mainly controlled by radiation (i.e., climate) and not by stand age [*Stagnitti et al.*, 1989]. Because these derived ET values are integrated whole-canopy fluxes, by definition, they include interception.

[11] These values were implemented as a factor into the α values determined through the measurements shown in Figure 2 and used to represent the effects of harvesting in a number of selected years. These large ET_h/ET_u ratios are in agreement with the rapid aspen regeneration reported by *Devito et al.* [2005] in the Boreal Plain, where suckers of trembling aspen exceeding 0.3 m in height were observed at the end of the first growing season, reaching 1 m in height by the end of the second growing season. This fast regeneration is also reported by *Whitson et al.* [2005], who observed that aspen reestablished quickly at all their harvested sites, reaching 2 m in height by the end of the third year after harvest.

2.1.2. Snowpack Dynamics

[12] Adequate modeling of snowpack accumulation and melt need particular consideration, as the snowpack's size and properties affect the timing of thaw in the soil and the amount of liquid present in the spring [*Bartlett et al.*, 2006]. Snowmelt was determined through the degree-day method, where daily snowmelt (m) is related to T_a and a melt factor (M) whenever T_a exceeds a threshold temperature ($T_{thr} = 0°C$):

$$m = M(T_a - T_{thr}), \tag{2}$$

where M (mm °C^{-1} d^{-1}) accounts for the effect of different factors that affect snow melting and varies with time. This factor was estimated using an empirical relationship derived for forested areas [*Kuusisto*, 1980]:

$$M = 10.4\frac{\rho_s}{\rho_w} - 0.7, \tag{3}$$

where ρ_s is snow density (kg m^{-3}) and ρ_w is water density.

[13] Snowpack density varies with time and is influenced by both the density of new snow ($\rho_{s_{\mathrm{new}}}$) and the compaction and settling of the existing snow [*Riley et al.*, 1972]. *Pomeroy et al.* [1998] found that for most parts of Canada the average density of fresh snow varies between 50 and 120 kg m^{-3}, a value that is required to estimate snow depth when water equivalent is known. The density of freshly fallen snow was estimated by [*Hedstrom and Pomeroy*, 1998]

$$\rho_{s_{\mathrm{new}}} = 67.9 + 51.3e^{T/2.6}. \tag{4}$$

[14] Over time, snowpack density increases because of different effects. The daily change of snowpack density with time is modeled with the empirical relationship used in the Canadian Land Surface Scheme (CLASS) model [*Verseghy*, 1991]:

$$\rho_s(t+1) = [\rho_s(t) - \rho_{s,\max}]e^{-0.24} + \rho_{s,\max}, \tag{5}$$

where $\rho_{s,\max}$ is determined by the following relationship with snow depth (z_{snow}, in m) [*Bartlett et al.*, 2006]:

$$\rho_{s,\max} = 450 - \frac{204.7}{z_{\mathrm{snow}}}[1 - e^{-(z_{\mathrm{snow}}/0.673)}], T_s < 0°\mathrm{C}, \tag{6}$$

where the 450 kg m^{-3} constant is replaced by 700 kg m^{-3} for an isothermal snowpack at 0°C (i.e., when melting occurs). After snow falls, ρ_s is recalculated as the weighted average of the previous density and that of freshly fallen

Table 1. ET Ratio for Harvested (ET_h) to Undisturbed (ET_u) Aspen, Within 6 Years of Harvesting[a]

Year	ET_h/ET_u
0	0.70
1	0.74
2	0.83
3	0.88
4	0.92
5	0.96
6	1.00

[a]The values are for winter harvest (P. D. Blanken, personal communication, 2010; S. K. Carey, unpublished data, 2010).

snow, as done in CLASS [*Verseghy*, 1991]. Additionally, after deposition, snow depth decreases by the compaction effect of snow age [*Singh et al.*, 2009; *Riley et al.*, 1972]:

$$\Delta z_{\text{snow}} = z_{\text{snow}} c_s \left(1 - \frac{\rho_s}{\rho_{s,\max}}\right), \tag{7}$$

where Δz_{snow} is compaction depth (m) and c_s is a settlement constant (m) that needs to be calibrated to measured snow depth [*Singh et al.*, 2009].

[15] This methodology was calibrated and validated with climatological data from Fort McMurray (Figure 3), as snowpack depth data were available from 1956 to 1998. During calibration (1956–1965), a constant of 250 kg m^{-3} was used in equation (6), as generally assumed [*Pomeroy et al.*, 1998], because the snow water equivalent (SWE) values obtained with 450 and 700 kg m^{-3} were too large, accounting for more than 50% of the yearly precipitation. During calibration, the settlement constant c_s was adjusted to 0.275 m. The SWE values obtained with this methodology were not compared to those from Environment Canada at Fort McMurray as they were derived through the use of the 10:1 rule (i.e., 10 mm of snow = 1 mm of SWE). The validation results of Figure 3 show that the simulation of daily snowpack dynamics is adequate and that the largest daily precipitation events are caused by rainfall. These large precipitation events occur simultaneously when the largest evapotranspiration rates are expected (June–July).

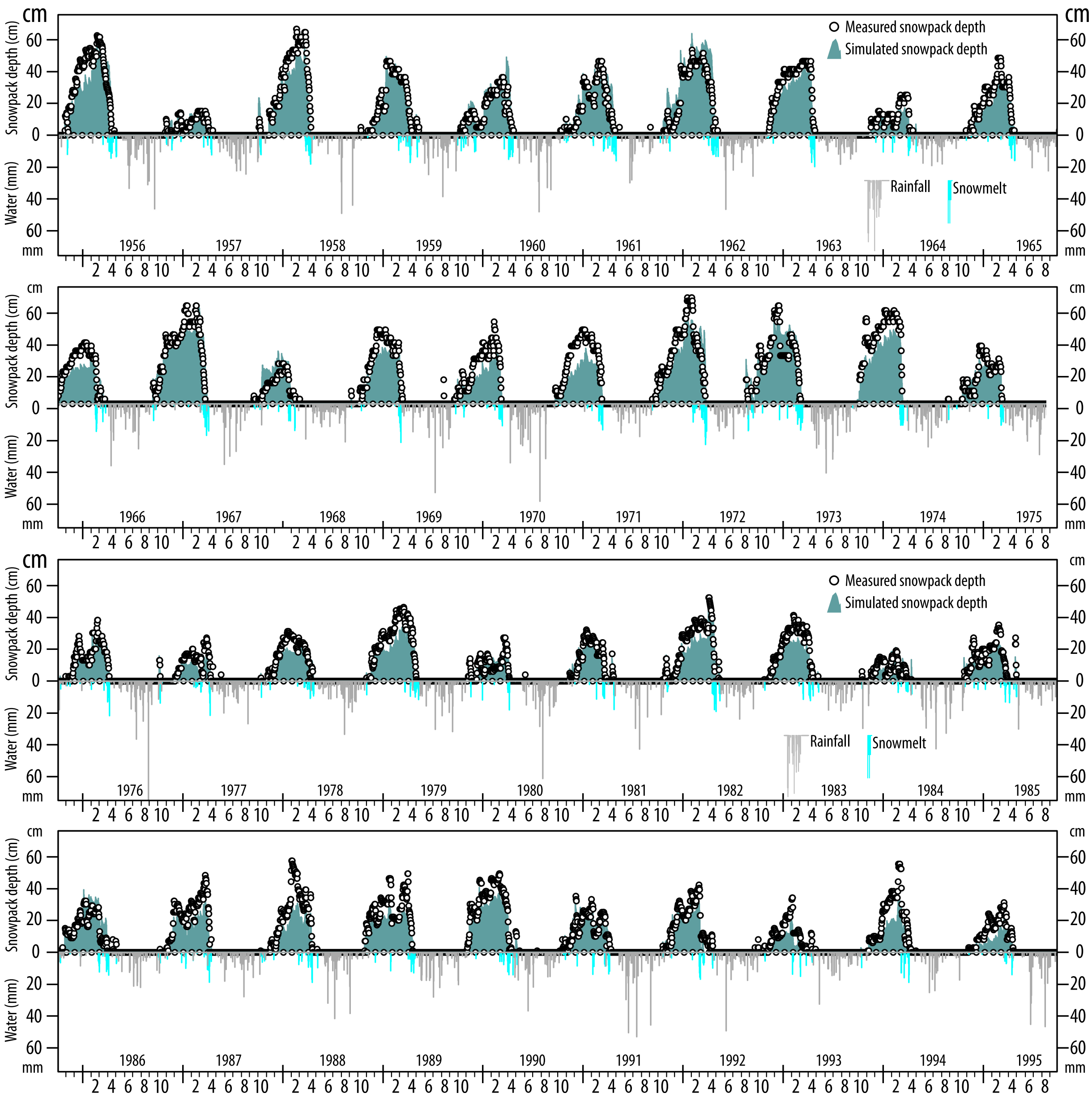

Figure 3. Calibration and validation of snowpack depth and snow water equivalent. Calibration was undertaken using the 1956–1965 period, while the remaining years were used for validation. Simulated snow depth values are shown with measured snow depth from the Fort McMurray climatological station. Measured rainfall at the station is also shown.

Sublimation was not considered in this work, as during snowfall the interception of snow by aspen (which is a deciduous tree) is expected to be low, and the highest rates of sublimation occur from intercepted snow [*Pomeroy et al.*, 1998]. However, the SWE values developed here would improve by including the prairie blowing snow model of *Pomeroy et al.* [1993].

2.1.3. Climatological Cycles

[16] The snow water equivalent obtained with this methodology was used to determine precipitation values, along with rainfall data on a daily basis. These values were aggregated on a yearly basis to represent the percentage of SWE to yearly precipitation, as illustrated in Figure 4, which also shows the normals (1971–2000) for both precipitation and reference evapotranspiration as well as the 5 year moving average of these two variables. A 5 year moving average was chosen because this is the approximate time that aspen takes to recover after harvesting occurs, thus helping to visualize wet and dry cycles related to aspen. It is expected that these periods will provide extreme cases on harvesting effects for both recharge and water table fluctuation, as a deeper water table and large soil moisture storage capacity are expected in dry cycles, while the opposite is expected to occur during wet cycles. The cyclic nature of climate in Alberta needs to be considered, as *Mwale et al.* [2009] found that these cycles can have periods of 4–8, 11, and 25 years.

2.2. Unsaturated Flow Modeling

[17] Daily soil moisture dynamics and fluxes at the water table were analyzed through unsaturated flow modeling on monolithic columns of 10 different materials and 4 different depths (2, 4, 6, and 12 m); these materials and depths were selected because they can be found on the heterogeneous landscape of the Boreal Plain. The *van Genuchten* [1980] relationships for sand, loamy sand, sandy loam, loam, and sand-clay-loam were developed from the parameters of *Carsel and Parrish* [1988]. The selection of materials was based on the surficial geology of the URSA (Figure 1), while the water table depths were based on those observed by *Smerdon et al.* [2008]. In addition, the soil properties determined in the boreal forest by *Cuenca et al.* [1997] as part of the Boreal Ecosystem-Atmosphere Study (BOREAS) from one fine-sand study site in Manitoba (BOREAS sand 1) and three sites in Saskatchewan consisting of sandy loam dominated by mature black spruce, silty loam dominated by mature aspen, and sand (BOREAS sand 1) dominated by old jack pine were also used. Borden sand was also employed on the basis of the parameters of *Si et al.* [1999]. These parameters were used in HGS to generate the corresponding tabular relationships of saturation versus relative hydraulic conductivity and saturation versus head (matric potential in the unsaturated zone; Figure 5).

2.2.1. Base Case Scenarios

[18] The soil columns were variably discretized at both the top and bottom, starting with 0.1 cm, and increased by a factor of 1.1 to reach a maximum spacing of 10 cm, while the water table was fixed at the bottom of each column. These options were selected because through a sensitivity analysis, it was found that this variable discretization provides efficient solution times and a more physically based representation of the water table. Base case scenarios (i.e., undisturbed aspen) were simulated using net daily climatological flux ($P - \mathrm{ET}$) as the top boundary condition and fixing the water table at 2, 4, 6, and 12 m in order to obtain fluxes at the water table (i.e., recharge and upward flux).

2.2.2. Harvesting Scenarios

[19] Harvesting years (1931, 1942, and 1970) were selected to represent the effect of harvesting on both wet and dry cycles. The first harvesting scenario (1931) represents the start of a wet cycle right after a dry one; the peak of this wet cycle occurs in 1936, whereas when harvesting occurs in 1942, the driest cycle on record is at its peak, with some of the lowest P/ET_0 ratios recorded as of 1940. The last harvesting scenario was selected to start in 1970, immediately after the end of a short dry cycle, and includes both the wettest cycle and the largest yearly precipitation.

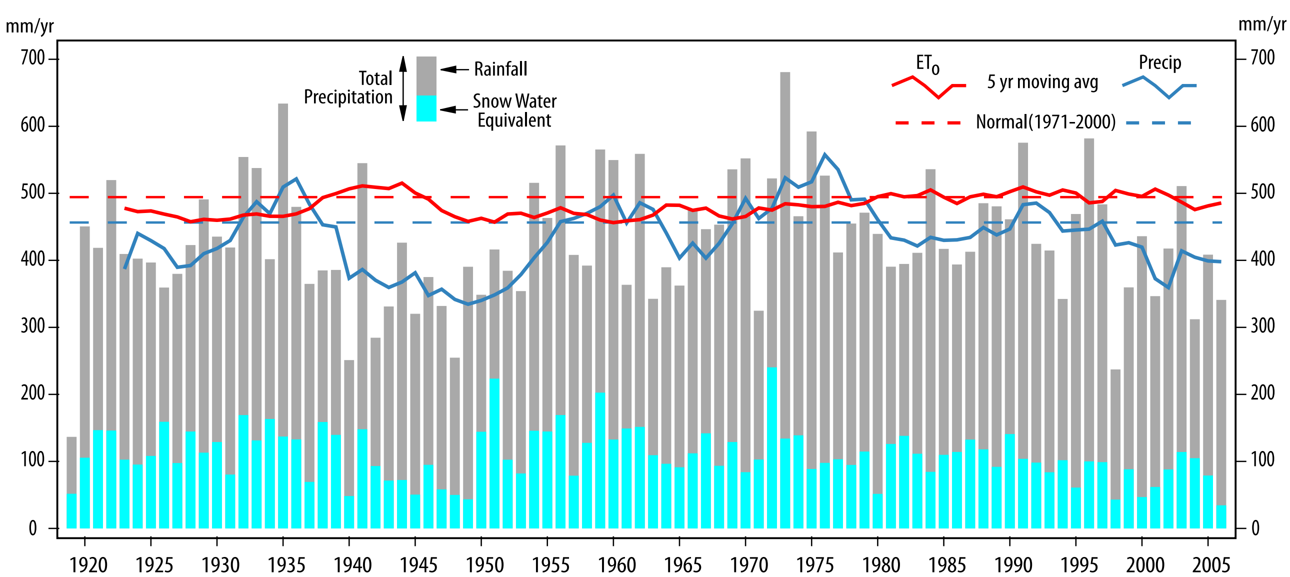

Figure 4. Yearly snow water equivalent, rainfall, and total precipitation at Fort McMurray. The 5 year moving average of both ET_0 and P is also shown, along with their respective normals (1971–2000).

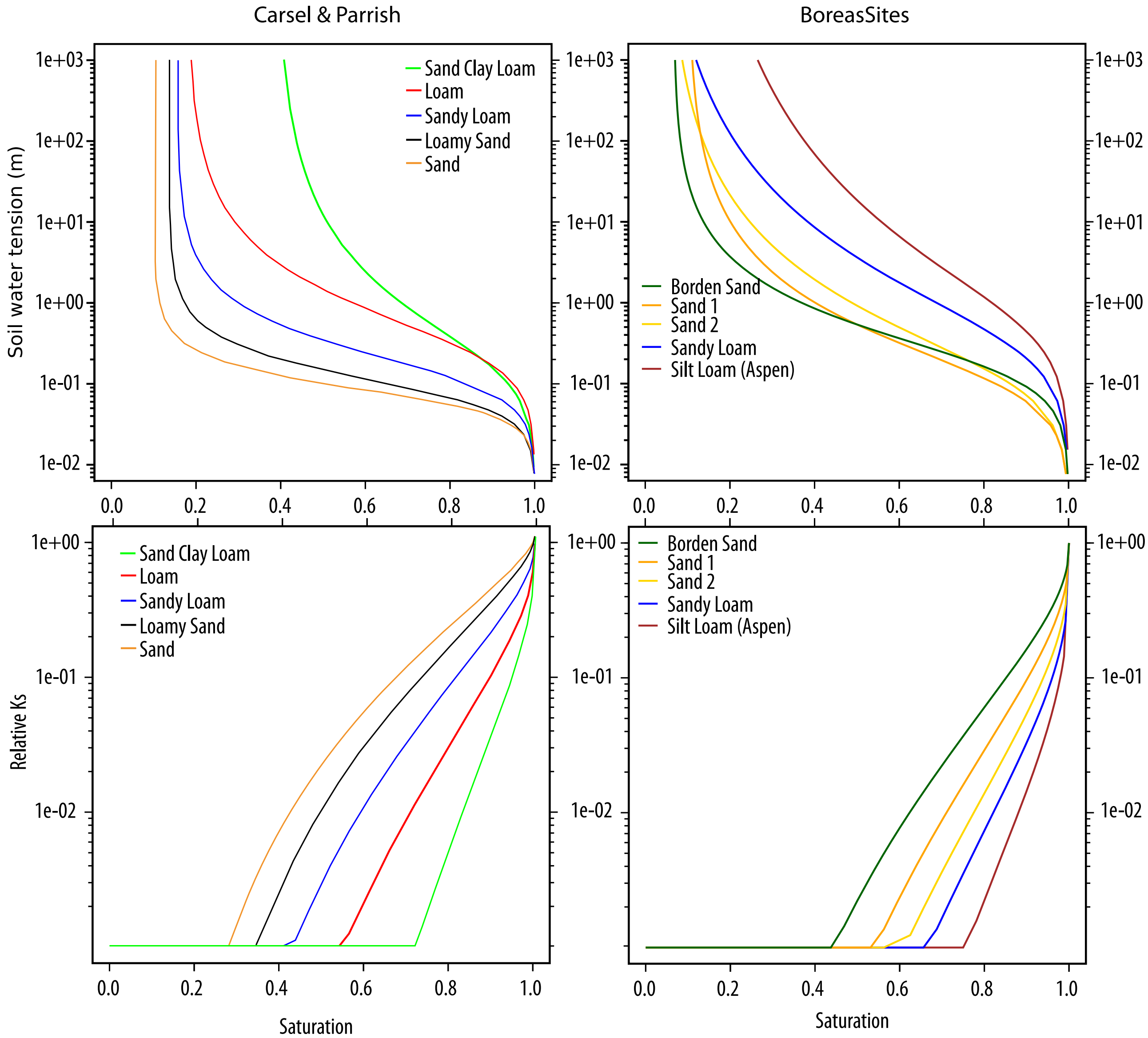

Figure 5. Saturation curves for the different materials used: (left) saturation matric head and (right) saturation-relative K_s. These curves are based on tabular values determined from the van Genuchten parameters of *Carsel and Parrish* [1988], *Cuenca et al.* [1997], and *Si et al.* [1999].

3. Results and Discussion

3.1. Base Case Scenarios

[20] The saturation profile for each depth and material along with the resulting fluxes at the water table were extracted for the 10 materials and the 4 depths used, although for illustrative purposes, only that of sandy loam is shown in Figure 6. These profiles illustrate how soil moisture impacts recharge because more water is kept within the soil when it has low saturation values; this impact is visible in Figure 6e for a 12 m profile, while the delay between precipitation events and recharge is noticeable if the fluxes at the water table for the four different depths are compared (Figure 6f).

[21] During the 1919–1934 period, a recharge of less than 5 mm month^{-1} is observed on the 12 m profile, increasing by the end of 1934 and peaking toward the end of 1935. For this period, upward flux was dominant toward the end of both 1926 and 1927 for the 2 m case, while for the other four depths used, the fluxes were downward (i.e., recharge) on these years. For this depth (2 m), significant upward flux (≈10 mm month^{-1}) occurs again toward the end of 1937, right after the presence of a large (≈50 mm month^{-1}) recharge flux. Although for the 2 m column recharge occurs during 1938–1940, upward flux is dominant, reaching its largest value in 1940, when upward flux is also observed on the 4 m column.

[22] The effect of the unsaturated zone thickness on recharge is evident during 1941–1963; for a 2 m thick unsaturated zone, there are three recharge peaks between 1941 and 1942, while recharge diminishes for the three remaining depths. During 1950, 1951, 1954, and 1955, there are recharge peaks for the 2 m column, reaching 50 mm month^{-1} in 1951; however, when the water table is

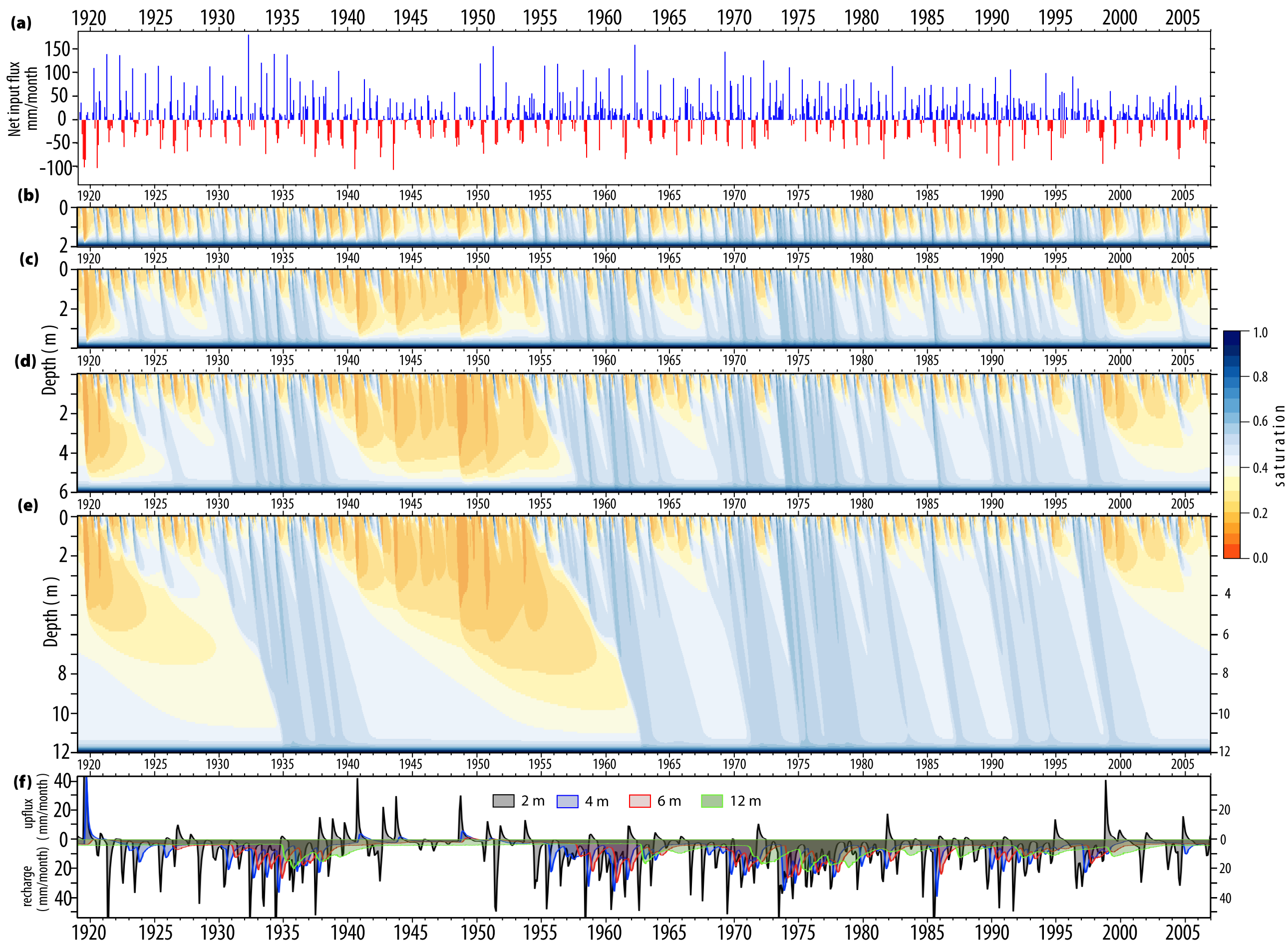

Figure 6. Daily simulation output on sandy loam for 1919–2006. (a) Net monthly atmospheric fluxes and soil moisture dynamics for column depths of (b) 2 m, (c) 4 m, (d) 6 m, and (e) 12 m. (f) Daily net fluxes at the water table aggregated on a monthly basis. A monthly aggregation was chosen for both net input fluxes and water table fluxes to improve interpretation.

4 m deep, it is not until the end of 1955 that recharge occurs. Recharge takes longer for the 6 m column, as it does not occur until late 1958, while for the 12 m case, recharge occurs in late 1963. As illustrated in the soil saturation profiles (Figures 6b–6e) different recharge events are needed to reduce soil moisture storage in order to produce recharge at the water table. The impact of a dry soil on fluxes at the water table can clearly be seen on the sandy loam saturation profiles of Figure 6, where it is noticeable how the soil is drying in the 1920s and starts to gain moisture in the 1930s. Because of this increase in soil moisture, the wetting front reaches the water table faster.

[23] The soil reaches its minimum water content in the mid 1950s for sandy loam (Figure 6e) because it started to dry in mid-1937 and did not start to gain moisture until 1954. As illustrated in Figure 6e, the recharge event of 1954 (which was caused by snowmelt) is reflected in the same year; however, for a water table located 4 m below ground, the recharge event of 1954 is added to that of 1955, and both are reflected at the water table toward the end of 1955. A series of precipitation surpluses are needed for moisture to reach the water table when it is at a depth of 6 m because recharge does not occur until late 1957. In the case of a 12 m deep water table, this effect is not visible until early 1963 (i.e., 9 year lag). To summarize, during the 13 years that the driest period in record lasted, both recharge and upward flux occurred for the shallowest water table (2 m), with snowmelt events being able to reach the water table (i.e., 1950 and 1951); in the case of a 4 m deep water table, no recharge occurs for approximately 13 years, while recharge is negligible for 15 years when the water table is located at 6 m. In the case of the deepest water table used, recharge still occurs during this period ($\approx$7 mm month^{-1}), taking approximately 19 years to increase after remaining constant since 1944.

3.1.1. Water Fluxes

[24] The simulated daily fluxes for all materials used were aggregated on a monthly basis to improve their interpretation, as illustrated in Figure 7. In the case of sand (Figure 7a), there is a strong interaction between atmospheric fluxes and the water table with no significant lag between positive input ($P >$ ET) on recharge and negative input (ET $> P$) on upward flux. However, the maximum recharge values when the water table is at 12 m reaches 20 mm month^{-1}, a value that is similar to that of a water table located at 4 and 6 m below the surface. When the water table is shallow (2 m), both recharge and upward flux can be larger than 40 mm month^{-1}. When finer textures are used, there is a variable

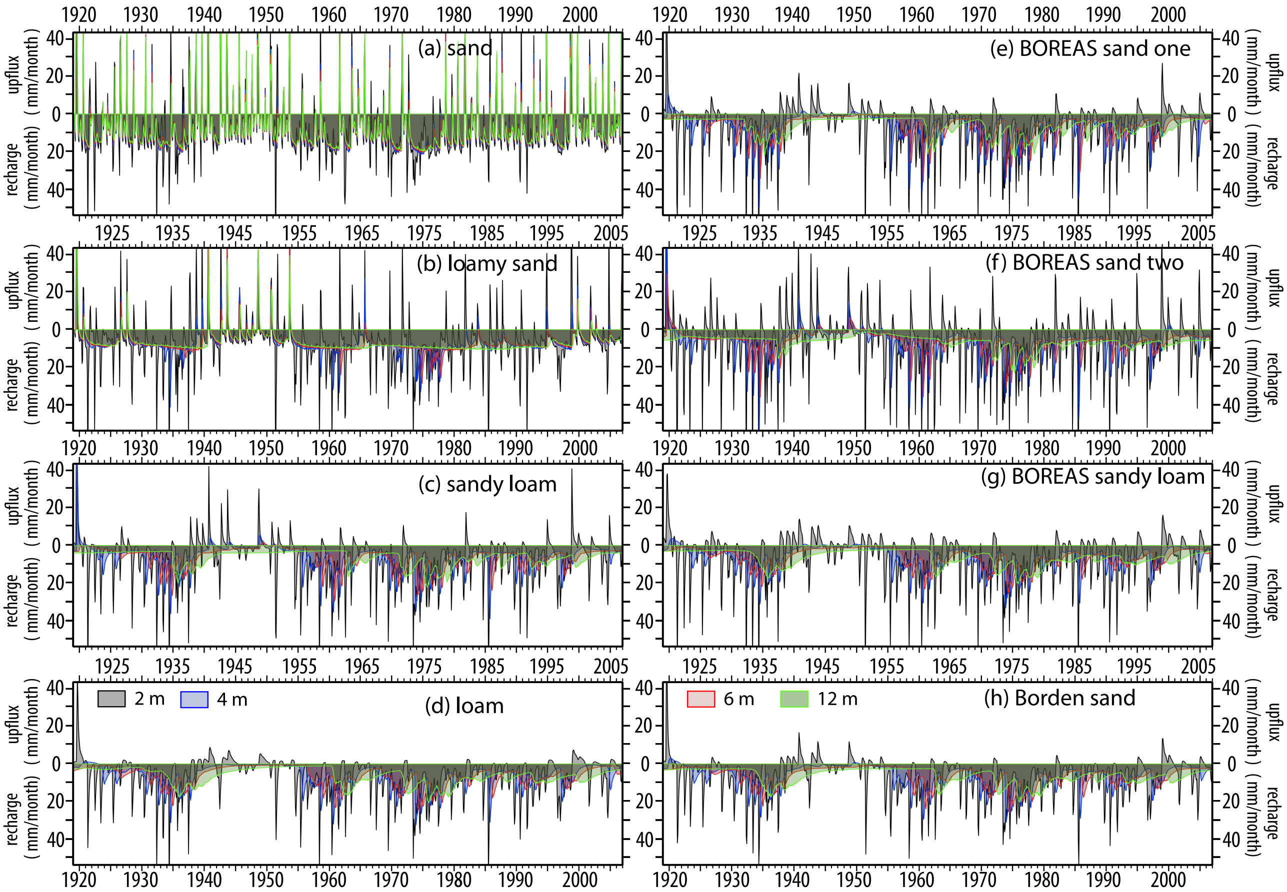

Figure 7. Monthly fluxes at the water table aggregated from daily values for the entire simulation period using four different water table depths (2, 4, 6, and 12 m) and eight different soil textures: (a) sand, (b) loamy sand, (c) sandy loam, (d) loam, (e) BOREAS sand 1, (f) BOREAS sand 2, (g) BOREAS sandy loam, and (h) Borden sand.

lag between positive inputs into the model and recharge that seems to be a function of water table depth. The fluxes at the water table for sandy loam and Borden sand behave in a similar fashion for the deepest water table (12 m), reaching a uniform recharge flux of around 5 mm month^{-1}. This flux is modified during a wet period (Figures 7c and 7h), reaching a maximum value of 20 mm month^{-1} around early 1936, corresponding to the first wet period (1931–1937); then in early 1964 and, finally, in mid-1972 it nearly reaches 20 mm month^{-1}, exceeding this value in 1976. For these two materials (sandy loam and Borden sand), it is in the 1970s that the monthly fluxes for the deepest case fluctuate, as they correspond to the wettest cycle in record (Figure 4). However, for a shallow water table (2 m), upward flux is different on Borden sand than on sandy loam because for sandy loam, upward flux reaches a value of 40 mm month^{-1} in late 1940, while it reaches approximately 15 mm month^{-1} at that same date for the Borden sand case.

[25] When the water table is shallow, upward flux occurs even on loam during the 1938–1954 period, reaching approximately 10 mm month^{-1} at the end of 1940 (Figure 7d). In the case of a 12 m deep water table, the maximum recharge value can be as high as 20 mm month^{-1} for all materials, except on loamy sand, which shows a consistent recharge rate of approximately 10 mm month^{-1}; for this depth, upward flux occurs only on sand and loamy sand (Figures 7a and 7b). The fluxes obtained with this water table depth (12 m) clearly show the lag between positive atmospheric influx and recharge when materials get finer, which can be observed with the peak recharge of 1936 for all materials except sand and loam sand.

3.1.2. Water Table Response

[26] A fixed water table depth was used to determine recharge and upward flux; however, this assumption needs to be verified. To achieve this, the mean daily flux at the water table obtained for the entire simulation length and for each material was determined and used as a lower boundary condition in each case to analyze how much the water table would fluctuate. Larger soil depths were required for these modeling experiments in order to avoid drying of the soil; accordingly, soil depths of 14, 16, 18, and 24 m were used to initialize the water table at 2, 4, 6, and 12 m, using a vertical discretization of 5 cm on all the experiments. The water table fluctuations obtained for sand, loamy sand, sandy loam, and loam are shown in Figure 8.

[27] For all materials and depths, the water table fluctuates in response to climate variation: in the case of sand (Figure 8), the water table oscillates around 3 m below surface before 1935, when it responds to the large precipitation registered in that year, rising (about 1.8 m deep) and then falling in response to the dry period of the 1940s, reaching a depth of approximately 5 m in 1954. The water

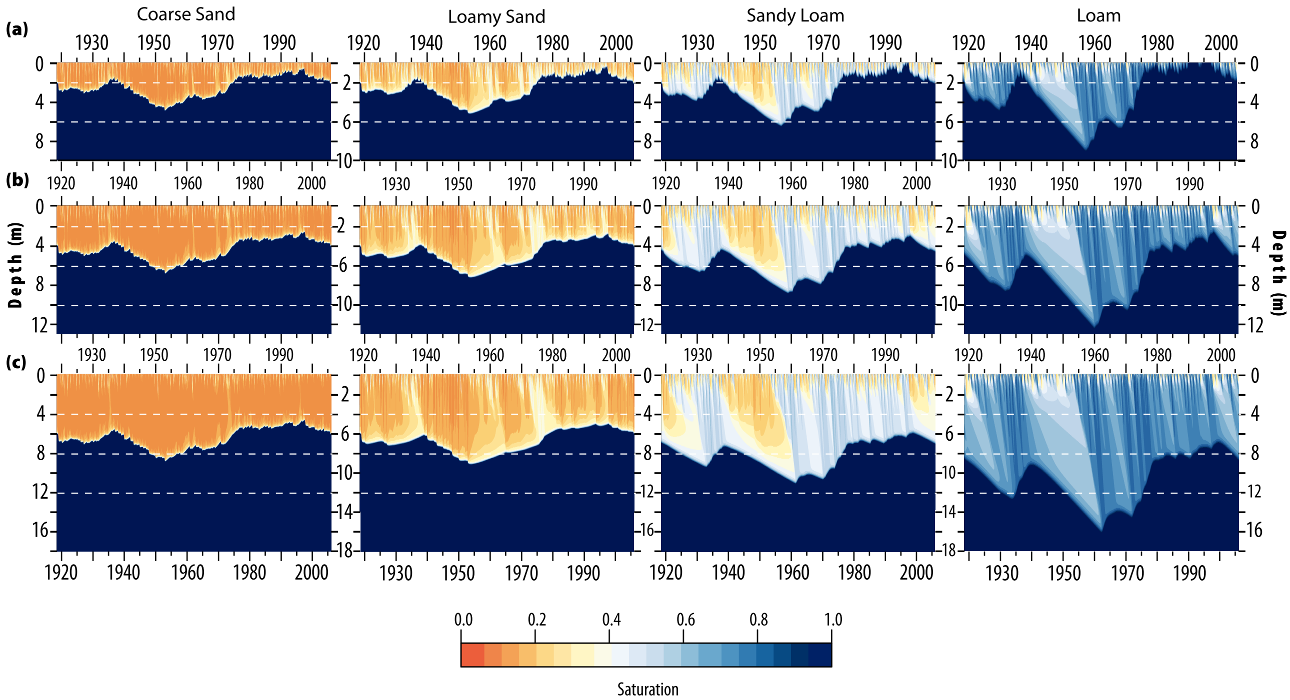

Figure 8. Long-term water table fluctuation for sand, loamy sand, sandy loam, and loam using three different initial depths: (a) 2 m, (b) 4 m, and (c) 6 m. The long-term recharge value obtained with a fixed water table for each case was used at the bottom of the soil columns to simulate the fluctuations.

table then rises again at a fairly steady pace (except for the response shown around 1962) up to the late 1970s, when it oscillates at a depth of 1.8 m. This response is observed on the other materials as well, except that on finer materials (i.e., Borden sand and sandy loam) the water table fall observed in the late 1930s is steeper, fluctuating up to 4 m, while on both sand and loamy sand this fluctuation was around 3 m. When finer materials are analyzed, the water table fluctuation observed in the 1940s is more dramatic: for loam (Figure 8), this fluctuation was around 8 m, while for sand clay loam (not shown) it reached 12 m. This rapid response can be explained by the capillary fringe of fine-textured material because the capillary fringe (and thus the zone of saturation) may extend for several meters above the water table [*Gillham*, 1984], explaining the fast response observed from 1975 onward, when the water table is closer to the surface.

[28] According to the fluctuations observed in Figure 8, the use of a fixed head lower boundary condition to represent the water table seems appropriate to determine fluxes at the water table on a long-term basis. It should be emphasized that the water table fluctuations observed in Figure 8 are not expected to be as pronounced because the outflow at the bottom of the profile would increase when the water table rises and decrease when the water table falls due to gradient variations. Consequently, the water table fluctuations of Figure 8 are extreme representations of a fluctuating water table.

3.2. Harvesting Scenarios

[29] The effect of harvesting on both water table fluxes and water table fluctuation was analyzed using the ET_h/ET_n ratios of Table 1. Harvesting is expected to affect both fluxes at the water table and water table depth, which because of the nature of the modeling approach used, are analyzed on a separate basis.

3.2.1. Effects on Water Fluxes

[30] The effects of harvesting on soil moisture dynamics and water fluxes at the water table for 1931, 1942, and 1970 are shown for loamy sand in Figures 9, 10, and 11, respectively. Loamy sand was selected, as the wetting and drying fronts in the soil profile and their relation to fluxes at the water table are more illustrative than for the other materials used. The 1931 aspen harvest occurs at the end of a dry period, as during and before 1931, $P < ET_0$ (based on a 5 year moving average) and $P < P_{normal}$ except for 2 years (Figure 4). It is in 1931 that the wet period starts, including the second largest precipitation event for the entire record, in 1935. The second harvest (1942) is simulated in the middle of a dry period, when $ET_0 > ET_{0_{normal}}$ and $P < P_{normal}$, extending up to 1958. Finally, the 1970 harvest occurs during the wettest period on record, including the largest yearly precipitation in 1973 and a year with small precipitation (1971), below the normal for about 100 mm (Figure 4).

[31] When harvesting occurs in 1931, the soil profile has a large moisture retention capacity, and under undisturbed conditions, recharge barely occurs in the second half of 1931 when the water table is 2 m deep, with a lag of approximately four months (Figures 9b and 9c). In the case of the 4 m profile (Figure 9d), the soil starts to gain moisture in early 1932 but not enough to generate a recharge event, which does not occur until January–February of 1934, thus having a lag of nearly 6 months, while for the 6 and 12 m profiles, the soil absorbs all moisture, hindering recharge.

[32] Although the net input fluxes do not seem to vary much when harvesting occurs (Figure 9a), they impact soil

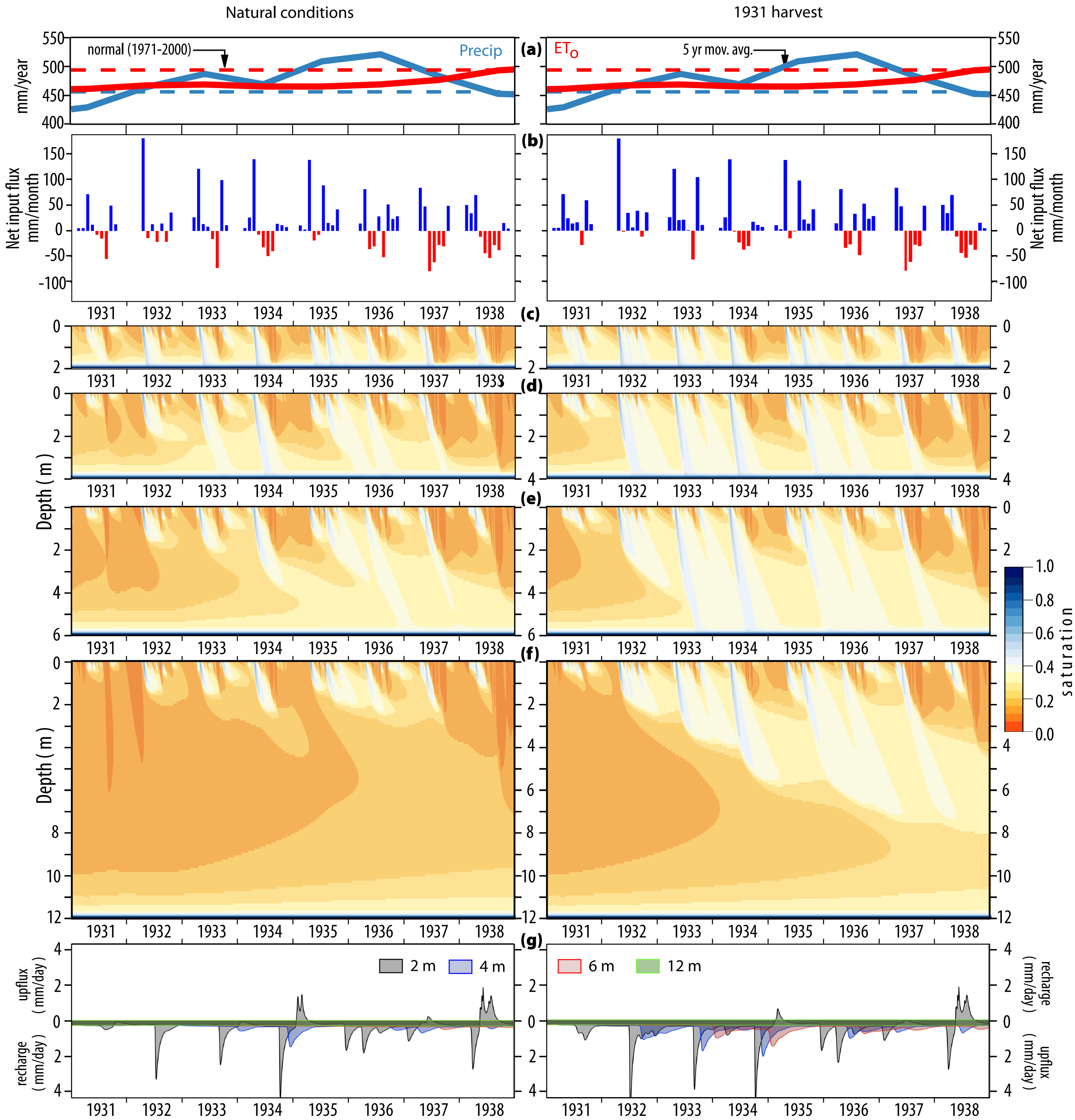

Figure 9. The 1931–1938 fluxes and soil moisture dynamics for the base case and harvesting scenarios on loamy sand. (a) The 5 year moving average and normals (1971–2000 average) for both precipitation and ET_0, (b) net monthly input fluxes, and soil moisture dynamics for soil profiles with depths of (c) 2 m, (d) 4 m, (e) 6 m, and (f) 12 m. (g) Resulting fluxes at the water table.

moisture dynamics in different manners, according to the thickness of the unsaturated zone. In the case of a 2 m deep water table, when harvesting occurs, recharge fluxes increase, but their timing does not change; however, for deeper water tables the fluxes increase, and their timing changes because recharge occurs earlier. When aspen is harvested in 1931, recharge occurs in late 1932 when the water table is 4 m deep, while no recharge occurs under undisturbed conditions at that time: the precipitation of 1932 provides enough water to reduce the soil's storage capacity up to a point where recharge occurs, facilitating its occurrence in the following years, thus moving the early 1935 recharge peak to late 1934 (Figure 9d). For the 6 and 12 m cases, the soil's dry fronts do not extend until early 1935 and early 1936, respectively. The daily fluxes for each case show that when the water table is 2, 4, and 6 m deep, the harvesting effects vanish at the seventh year after harvest. When the water table is at a depth of 12 m, the effects of harvesting on soil moisture are not strong enough to modify the fluxes at the water table (Figure 9f).

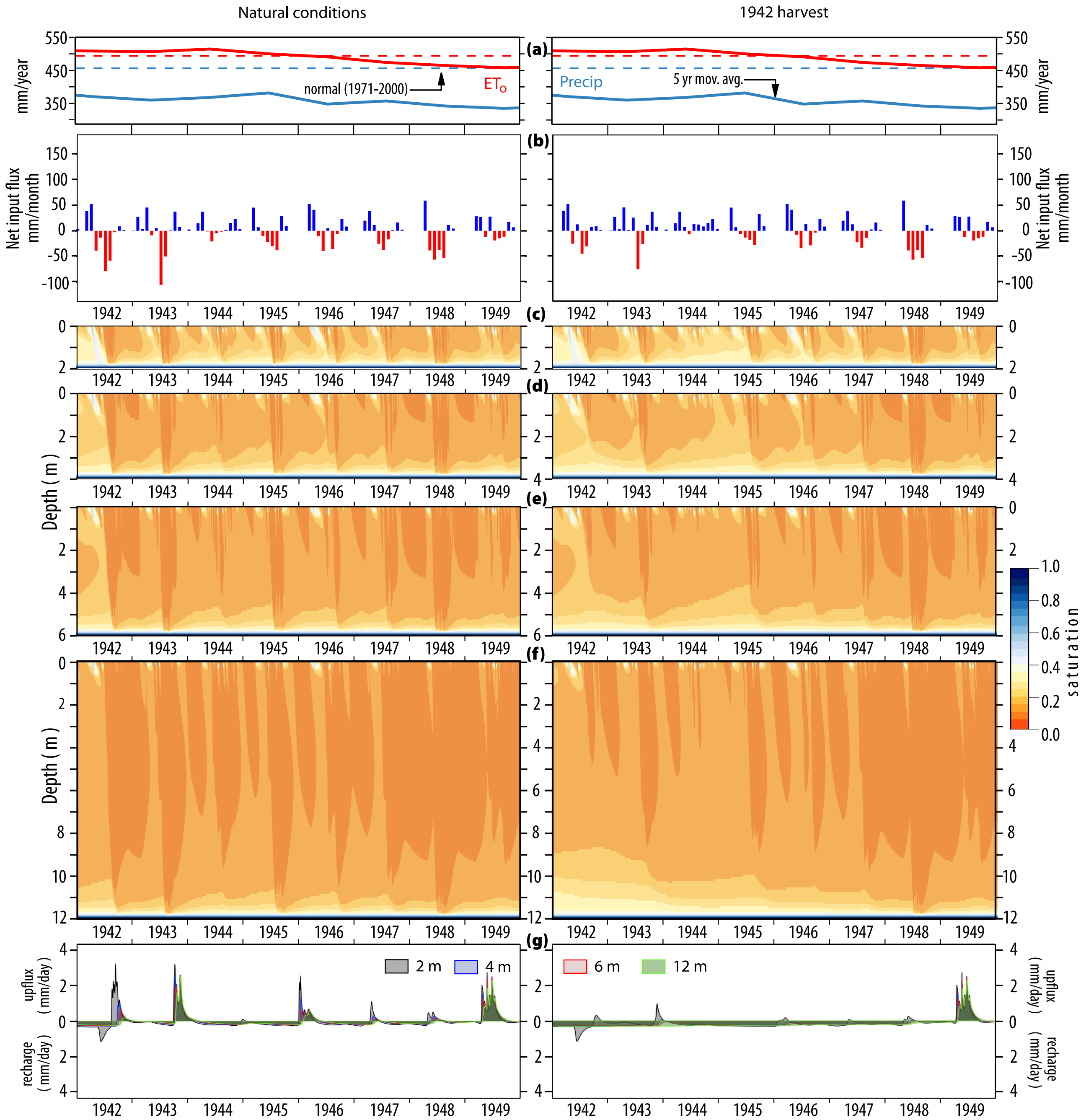

Figure 10. The 1942–1949 fluxes and soil moisture dynamics for the base case and harvesting scenarios on loamy sand. (a) The 5 year moving average and normals (1971–2000 average) for both precipitation and ET_0, (b) net monthly input fluxes, and soil moisture dynamics for soil profiles with depths of (c) 2 m, (d) 4 m, (e) 6 m, and (f) 12 m. (g) Resulting fluxes at the water table.

[33] The delay of harvesting effects on fluxes at the water table at both monthly and yearly scales in different wetness periods is shown in Figure 12, where the lag between harvesting effects on fluxes at the water table is illustrated for all materials used. When harvesting occurs on sand in 1931, its effect is visible toward the end of that same year, and its magnitude is quite similar for the four depths under study; however, for the other materials, the effect of harvesting peaks on the year after harvest for water table depths of 2 and 4 m (i.e., 1932). In the case of loamy sand and a water table depth of 6 m, the effect of harvesting peaks after 4 years of harvesting, as similarly observed for sandy loam when the water table is 12 m deep. For this case, the effects of harvesting seem to disappear toward the end of the eighth year.

[34] During a dry period (1942–1949, Figure 4), where the 5 year moving averages of P and ET_0 were lower and larger than their respective normals (Figure 4), the response to harvesting on sand is identical for all soil depths; however, this difference needs further consideration, as it does not reflect an increase in recharge. For loamy sand, the impact of harvesting is reflected in less water being taken

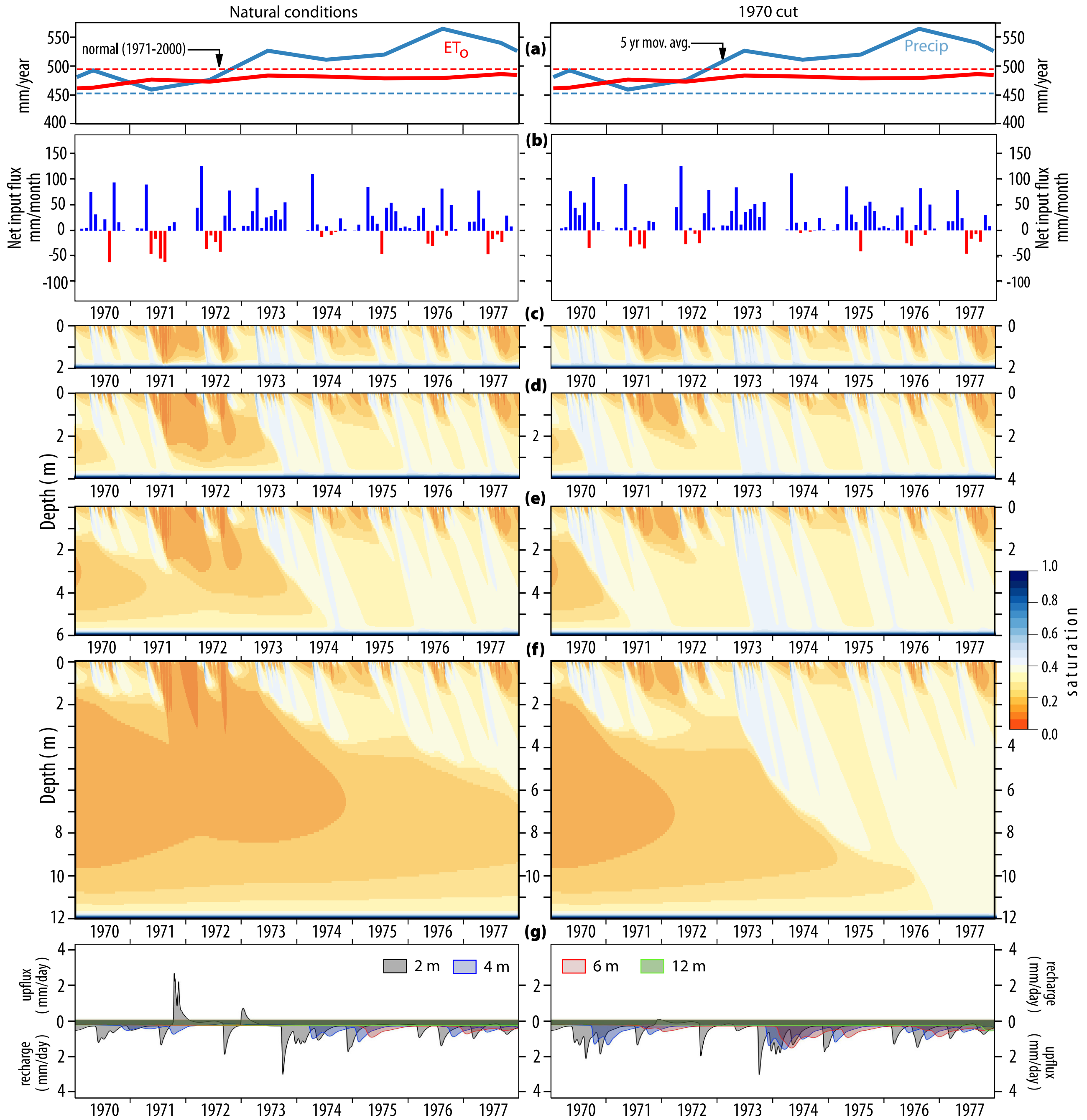

Figure 11. The 1970–1977 fluxes and soil moisture dynamics for the base case and harvesting scenarios on loamy sand. (a) The 5 year moving average and normals (1971–2000 average) for both precipitation and ET$_0$, (b) net monthly input fluxes, and soil moisture dynamics for soil profiles with depths of (c) 2 m, (d) 4 m, (e) 6 m, and (f) 12 m. (g) Resulting fluxes at the water table.

from the water table (i.e., upward flux, Figure 10g) in order to satisfy the aspen's water demand (ET). From the fluxes shown in Figure 7, this situation applies to all the materials used when harvesting occurs in 1942. The effects of harvesting fade toward the end of the eighth year, although they are still present. However, these effects are not expected to raise the water table because the impact of harvesting on a dry cycle is reflected by less water being taken by vegetation from the water table. This is caused by the large moisture storage capacity of the soil even with a shallow water table (Figures 10c and 10d).

[35] The last harvesting scenario occurs in 1970 and includes the wettest year on record (1973, Figure 4), reaching nearly 700 mm; in fact, during this year the net monthly atmospheric fluxes are positive for all months, although 1971 and 1972 were years with large negative atmospheric fluxes (Figure 11a). In fact, upward flux occurred in late 1971 and early 1972 on a shallow water table because of the large evaporative fluxes of 1971 (Figure 11g). When harvesting occurs in 1970, the 1971 upward flux is reduced and actually transformed into recharge, while for the remaining years, recharge is increased, but

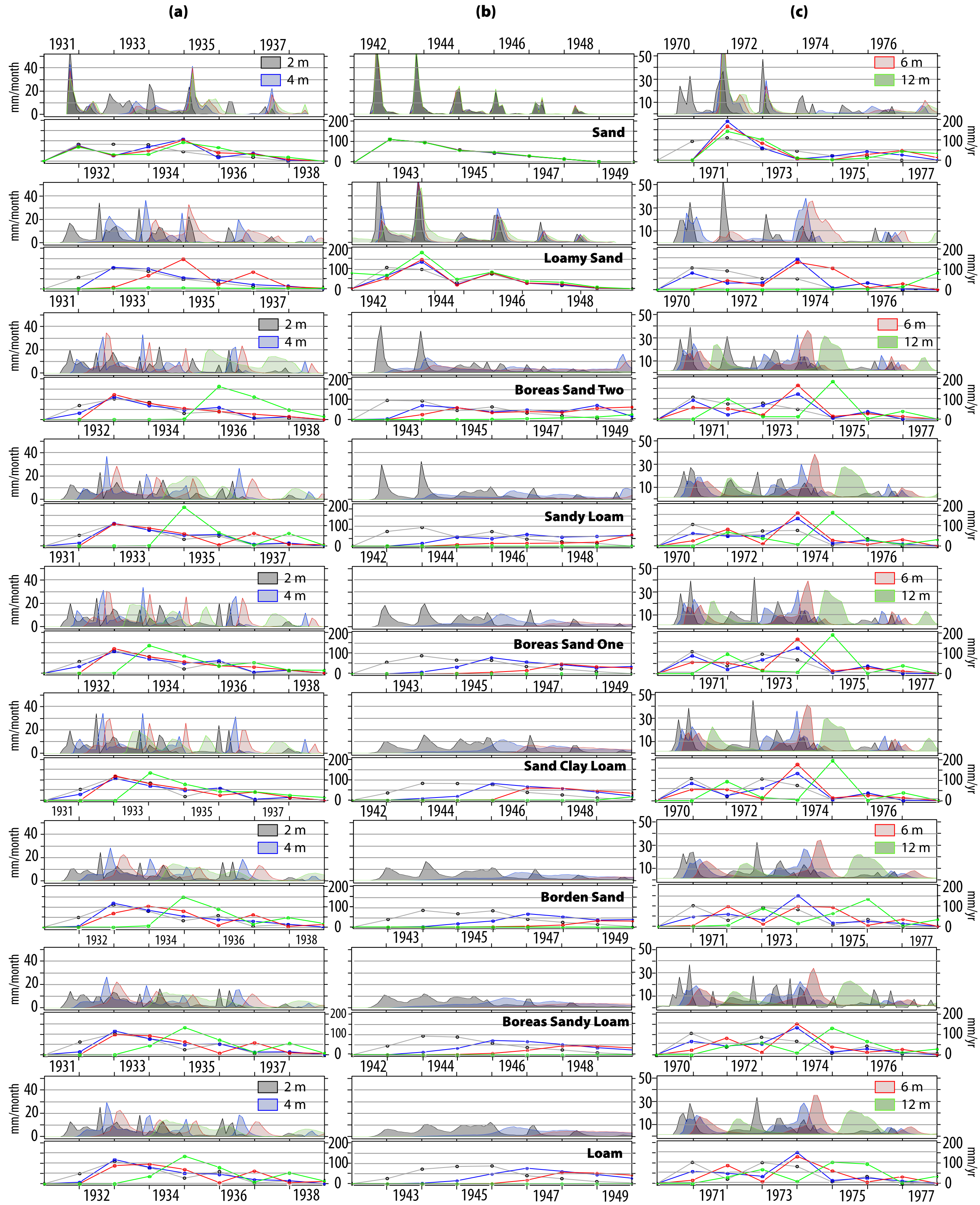

Figure 12. Flux differences on both a monthly and yearly basis between undisturbed aspen and harvesting scenarios for (a) 1931, (b) 1942, and (c) 1970 on nine different soil textures.

not its timing. The large precipitation of 1973 increased soil moisture, which in turn increased recharge for the shallowest water table; the timing of recharge was only modified when the water table is at a depth of 4 and 6 m, as it occurs approximately 5 months earlier for 4 m and almost a year earlier for the second case. Apparently, the effect of harvesting vanishes within 8 years for all materials except for the deepest water table on loamy sand (Figure 7c). For sand, the effect of harvesting is visible in the same year of harvesting for a 2 m deep water table, and 1 year later for the three remaining depths (Figure 7c). The other eight materials show the effect of harvesting in the same year that harvesting occurs when the water table is 2 and 4 m deep and even when it is at a depth of 6 m in the cases of sandy loam, loam, and sand clay loam. When harvesting occurs in 1970, the peak manifestation of its effect is visible after 1 year for a 2 m deep water table. However, for the case of water tables located at depths of 4 and 6 m, the peak shows toward the end of the fourth year after harvesting. The effect of harvesting on recharge takes longer to reach its peak for the deepest water table used, as it takes about 5 years to show, although in the case of sandy loam, it actually peaks in the eighth year (Figures 11g and 7c).

[36] From these results, it appears that in order to estimate the effect of harvesting on fluxes at the water table, not only is preceding precipitation important but also water table depth, soil texture, and whether harvesting occurs during a wet or a dry cycle. In addition, the flux differences at the water table caused by aspen harvesting will also affect water table depth, as discussed in section 3.2.2.

3.2.2. Effects on Water Table

[37] Section 3.2.1 showed that harvesting increases soil moisture, eventually increasing recharge; accordingly, the water table is expected to rise when more water reaches the aquifer. The same years used to analyze the effect of aspen harvesting on water fluxes (1931, 1942, and 1970) are used to study its effect on water table fluctuation, using the same fluxes at the bottom of the columns as when the water table fluctuations for the undisturbed scenarios were analyzed. Thus, the water table fluctuations of Figure 8 represent the undisturbed scenarios.

[38] When harvesting occurs in 1930, the water table depth in that year varies according to the selected initial water table depth and texture: an initial water table depth of 2 m was located at a depths of approximately 2.5, 3.5, 4, and 4.5 m for sand, loamy sand, sandy loam, and loam, respectively, in 1930 (Figure 8a). However, for this same case (e.g., 2 m initial depth) in 1938 the water table was located at approximately 1 m for all textures used (Figure 8a). Under undisturbed conditions, the water table starts to rise in 1930, and its rising rate increases when harvesting occurs, as more water reaches the water table. When harvesting occurs in 1931, the water table is expected to additionally rise by approximately 1 m in sand (compared to the base case), and its responses for the four different initial depths used are similar (Figure 13b).

[39] The observed water table response is different than the response observed on fluxes, as fluxes show larger increases even in the harvesting year (Figure 13a). For loamy sand, the 1931 harvesting effect on water table rise is delayed depending on its depth: for the 2 m case, the water table rises by approximately half a meter toward the first half of the year after harvest occurred (i.e., 1.5 year lag). This lag increases to 2.5 years for the 4 m case and to nearly 3.7 years for a 6 m deep water table; for the deepest water table, there is a small effect toward the end of the sixth year after harvest (approximately 0.1 m). The rising rate of the water table is larger for finer materials, although it takes longer to be noticed because for loam the soil column completely saturates on the three water table depths used (Figure 13a). Saturation of the profile occurs on the shallowest water table 3 years after harvest when the water table was approximately 4 m deep and 5 years when the water table was approximately 5 m deep (Figure 13a).

[40] When harvesting occurs in 1942, the effects on water table fluctuation are smoother than those observed in 1931, particularly for fine materials (Figure 14). In the case of sand, the water table response is similar when harvesting occurs in 1942 and in 1931; however, the water table response starts to differ for loamy sand because for the four depths used, the response is similar, becoming noticeable even at the end of the harvesting year. In the case of sandy loam, the water table elevation is affected only on the shallowest case (3 m deep in 1942, Figure 8a), reaching a maximum difference of 1 m, while for the 4 m case this response reaches a maximum value of 0.3 m; for the other two depths used the harvesting effect is indiscernible. The effect of harvesting is more significant in the case of loam because for the shallowest case the water table increases almost 1.5 m toward the end of the seventh year after harvest and nearly 0.5 m in that same year for the 4 m case.

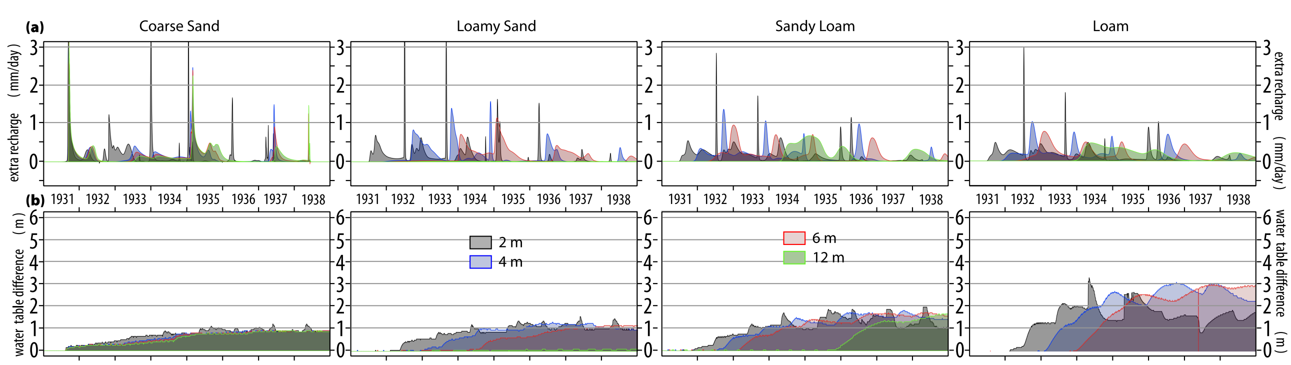

Figure 13. Effects of aspen harvesting on (a) daily fluxes and (b) water table elevation when harvesting occurs in 1931.

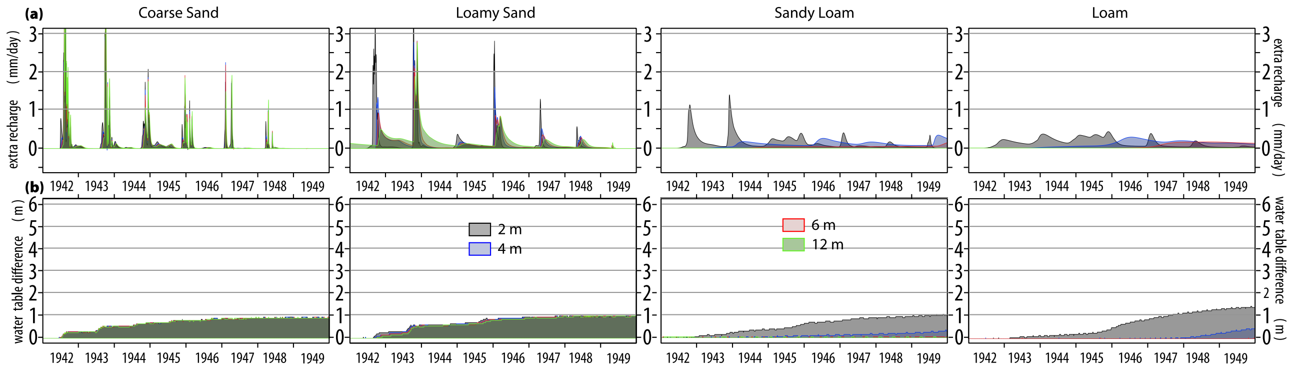

Figure 14. Effects of aspen harvesting on (a) daily fluxes and (b) water table elevation when harvesting occurs in 1942.

[41] The last harvesting scenario (1970) is interesting because the shallowest water table responds toward the end of the harvesting year (Figure 15). Similarly to the previous scenarios, the response is more pronounced on finer materials, and the effect of the largest precipitation event on record (1973, Figure 4) is also more pronounced on them. In the case of sand, the maximum response for all depths is approximately 1 m, with no significant lags for the depths used. The lag between harvesting and water table response starts to be appreciated on loamy sand: for the shallowest case, the water table depth decreases by 0.5 m toward the end of the harvesting year, while for the 4 m case the water table responds at the end of the second year after harvesting, by only 0.25 m. There is no discernible response on the third case because the water table is about 10 m deep (Figure 8). This occurs because when the water table is located at a depth of 6 m, the soil profile gains moisture due to harvesting (Figure 11e), but recharge barely increases (Figures 11g and 12c): when the vadose zone thickens, more water is stored in the soil (Figure 11g). This increase in soil moisture is required for precipitation to become recharge, which is noticeable for the large precipitation recorded in 1973, as during 10 months the monthly net atmospheric fluxes were positive (Figure 11b). In fact, the large amount of precipitation of 1973 causes the water table to rise in the same year for the shallowest water table on loamy sand, sandy loam, and loam, with a delay of approximately half a year for deeper water tables. Again, the response is larger on loam because the soil column saturates even for the shallowest case, with a fast response of nearly 3.5 m during 1973; this response has a lag of 1 and 2 years for the initial depths of 4 and 6 m, when the water table was located at 9 and 13 m below surface in 1973 (Figures 8b and 8c). The peak response for these two cases occurred 5 and 6 years after harvesting, causing the water table to rise by approximately 3 m.

[42] While interpreting the effects of harvesting shown in Figures 13, 14, and 15, it should be kept in mind that aspen harvesting impacts both fluxes at the water table and its elevation. Thus, the one-dimensional approach used in this work simplifies what occurs in reality because both recharge and upward flux are related to water table fluctuation. When recharge occurs, the water table is expected to rise, which in turn increases the probability of net positive atmospheric fluxes becoming recharge; however, when upward flux occurs, the water table falls, increasing the soil's storage capacity. When the water table rises, the gradient increases, and a larger flux than the long-term mean recharge flux used exits the water columns of these experiments; accordingly, the reported water table fluctuations represent an extreme case.

[43] The simulated fluctuation and delay of harvesting effects on the water table are in agreement with those observed in experimental catchments [e.g., *Peck and Williamson,* 1987; *Ruprecht and Schofield,* 1991]. However, the simulated effects are not as pronounced because there is no land use change and because aspen suckers regenerate fast, with ET rates reestablishing in 6 years. Nevertheless, these

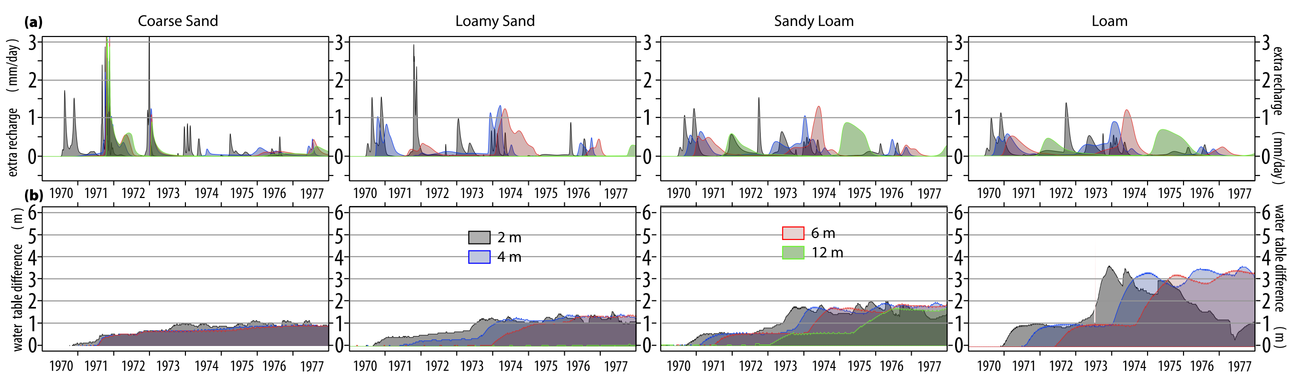

Figure 15. Effects of aspen harvesting on (a) daily fluxes and (b) water table elevation when harvesting occurs in 1970.

simulations need to be complemented by long-term studies of harvesting impacts in aspen-dominated catchments on the Boreal Plain, as pointed out by *Devito et al.* [2005].

4. Conclusions

[44] The vadose zone plays an important role on the Boreal Plain region, where both the subhumid climate ($P \leq ET_0$) and the deep glacial sediments result in large available soil storage capacity. In order to understand groundwater recharge dynamics and the effect of forestry activities on recharge, daily soil moisture dynamics and fluxes at the water table were analyzed through unsaturated flow modeling using monolithic columns of different materials and depths representative of the Boreal Plain heterogeneous landscape.

[45] The developed soil moisture profiles illustrate how the soil's storage capacity impacts recharge, as more water is kept within the soil when it has low saturation values, particularly for deep water tables. Strong interaction between shallow water tables (i.e., 2 m) and atmospheric variability is observed for all materials, an interaction that is reduced when the vadose zone thickens, particularly after a dry cycle, as a series of positive net atmospheric fluxes are needed to reduce soil moisture storage for recharge to occur. During the driest cycle on record, recharge was constant ($\approx$7 mm month^{-1}) for 19 years when the water table was located at a depth of 12 m in medium- and fine-textured soils, increasing only after the soil gained enough moisture to allow the wetting fronts to become recharge. On the basis of the undertaken simulations, it is expected that near Fort McMurray the maximum monthly recharge values will reach 20 mm month^{-1}, except in loamy sand, where recharge is only expected to reach 10 mm month^{-1}. On a short-term basis, these values are steadier on sand and loamy sand, while for finer materials they represent peak values. In addition, climate variability also affects the water table elevation, with major impacts on finer materials, particularly on shallow water tables because of their capillary fringe.

[46] The effect of harvesting on different climatological periods was analyzed for 1931, 1942, and 1970, as in 1942 and 1970 the driest and wettest cycles on record started. According to the results obtained in this work, harvesting does not have a negative effect when it occurs during a dry cycle, as upward flux is reduced and the water table is not expected to significantly rise even when it is located at a depth of 2 m. However, when the cycles get wetter the impacts can be significant and not immediate, eventually saturating the soil as the water table is shallower. This negative effect increases when soil textures get finer: on loam, the water table rises with a fast response of nearly 3.5 m.

[47] Overall, the water table is expected to rise between 1 and 3.5 m depending on soil texture and climatological conditions. The lag between harvesting and water table response varies from 1 year for shallow water tables to five years for a sandy loam texture when the water table is located at a depth of 12 m. However, this response can peak 2 years after harvest because of wetter conditions and shallower water tables caused by harvesting, thus enhancing recharge of posterior precipitation events.

[48] Although aspen regenerates quickly after harvesting, this activity influences soil moisture dynamics and, consequently, groundwater recharge and water table elevation. The effects of aspen harvesting are more pronounced during wet cycles, and the development of forestry activities on the Boreal Plain should consider not only preceding precipitation but also water table depth, soil texture, and whether harvesting occurs during a wet or a dry cycle. The interaction of these factors needs to be considered in order to develop sustainable forestry plans and avoid waterlogging conditions.

[49] **Acknowledgments.** We thank R. Therrien, E. A. Sudicky, and R. McLaren for allowing us use of the HydroGeoSphere code and for the support provided for its use.

References

Alila, Y., and J. Beckers (2001), Using numerical modelling to address hydrologic forest management issues in British Columbia, *Hydrol. Processes*, *15*, 3371–3387.

Allen, R. G. (2000), Using the FAO-56 dual crop coefficient method over an irrigated region as part of an evapotranspiration intercomparison study, *J. Hydrol.*, *229*, 27–41.

Amiro, B., et al. (2006), Carbon, energy and water fluxes at mature and disturbed forest sites, Saskatchewan, Canada, *Agric. For. Meteorol.*, *136*(3-4), 237–251.

Baldocchi, D. D., B. B. Hicks, and T. P. Meyers (1988), Measuring biosphere-atmosphere exchanges of biologically related gases with micrometeorological methods, *Ecology*, *69*(5), 1331–1340.

Bartlett, P. A., M. D. MacKay, and D. L. Verseghy (2006), Modified snow algorithms in the Canadian Land Surface Scheme: Model runs and sensitivity analysis at three Boreal forest stands, *Atmos. Ocean*, *43*, 207–222.

Blanken, P., T. Black, P. Yang, H. Neumann, Z. Nesic, R. Staebler, G. Den Hartog, M. Novak, and X. Lee (1997), Energy balance and canopy conductance of a boreal aspen forest: Partitioning overstory and understory components, *J. Geophys. Res.*, *102*(D24), 28,915–28,927, doi:10.1029/97JD00193.

Blanken, P. D., T. A. Black, H. H. Neumann, G. den Hartog, P. C. Yang, Z. Nesic, R. Staebler, W. Chen, and M. Novak (1998), Turbulent flux measurements above and below the overstory of a boreal aspen forest, *Boundary Layer Meteorol.*, *89*(1), 109–140.

Blanken, P. D., T. A. Black, H. H. Neumann, G. den Hartog, P. C. Yang, Z. Nesic, and X. Lee. (2001), The seasonal water and energy exchange above and within a boreal aspen forest, *J. Hydrol.*, *245*, 118–136.

Bosch, J. M., and J. D. Hewlett (1982), A review of catchment experiments to determine the effect of vegetation changes on water yield and evapotranspiration, *J. Hydrol.*, *55*(1), 3–23.

Buttle, J., I. F. Creed, and J. W. Pomeroy (2000), Advances in Canadian forest hydrology 1995–1998, *Hydrol. Processes*, *14*, 1551–1578.

Carsel, R. F., and R. S. Parrish (1988), Developing joint probability distributions of soil water retention characteristics, *Water Resour. Res.*, *24*, 755–769, doi:10.1029/WR024i005p00755.

Clark, R. B., I. F. Creed, and G. Z. Sass (2009), Mapping hydrologically sensitive areas on the Boreal Plain: A multitemporal analysis of ERS synthetic aperture radar data, *Int. J. Remote Sens.*, *30*(10), 2619–2635, doi:10.1080/01431160802552819.

Cuenca, R. H., D. E. Stangel, and S. F. Kelly (1997), Soil water balance in a boreal forest, *J. Geophys. Res.*, *102*(D24), 29,355–29,365, doi:10.1029/97JD02312.

Devito, K. J., I. F. Creed, and C. J. D. Fraser (2005), Controls on runoff from a part harvested aspen-forested headwater catchment, Boreal Plain, Canada, *Hydrol. Processes*, *19*, 3–25.

Dubé, S., and A. P. Plamondon (1995), Watering up after clear-cutting on forested wetlands of the St. Lawrence lowland, *Water Resour. Res.*, *31*(7), 1741–1750, doi:10.1029/95WR00427.

Elliott, J. A., B. M. Toth, R. J. Granger, and J. W. Pomeroy (1998), Soil moisture storage in mature and replanted sub-humid boreal forest stands, *Can. J. Soil Sci.*, *78*(1), 17–27.

Ferone, J., and K. J. Devito (2004), Shallow groundwater surface water interactions in pond peatland complexes along a Boreal Plains topographic gradient, *J. Hydrol.*, *292*, 75–95, doi:10.1016/j.jhydrol.2003.12.032.

Gillham, R. W. (1984), The capillary fringe and its effect on water-table response, *J. Hydrol.*, *67*, 307–324.

Grant, R. F., A. Barr, T. Black, H. A. Margolis, A. L. Dunn, J. Metsaranta, S. Wang, J. McCaughey, and C. A. Bourque (2009), Interannual variation in net ecosystem productivity of Canadian forests as affected by regional weather patterns—A Fluxnet-Canada synthesis, *Agric. For. Meteorol.*, *149*, 2022–2039.

Hamon, R. W. (1963), Computation of direct runoff amounts from storm rainfall, in *Symposium on Theoretical Studies and Practical Methods of Forecasting the Yield of Rivers for Both Long and Short Terms (Except Floods), IAHS Publ.*, *63*, 25–62.

Hedstrom, N. R., and J. W. Pomeroy (1998), Measurements and modelling of snow interception in the boreal forest, *Hydrol. Processes*, *12*, 1611–1625.

Hogg, E. H., J. P. Brandt, and B. Kochtubajda (2002), Growth and dieback of aspen forests in northwestern Alberta, Canada, in relation to climate and insects, *Can. J. For. Res.*, *32*, 823–832.

Kristensen, K. J., and S. E. Jensen (1975), A model for estimating actual evapotranspiration from potential evapotranspiration, *Nord. Hydrol.*, *6*, 170–188.

Kuusisto, E. (1980), On the values and variability of degree-day melting factor in Finland, *Nord. Hydrol.*, *11*, 235–242.

Landhäusser, S., U. Silins, V. J. Lieffers, and W. Liu (2003), Response of *Populus tremuloides, Populus balsamifera, Betula papyrifera*, and *Picea gauca* seedlings to low soil temperature and water-logged soil conditions, *Scand. J. For. Res.*, *18*, 391–400.

Marcotte, P., V. Roy, A. Plamondon, and I. Auger (2008), Ten-year water table recovery after clearcutting and draining boreal forested wetlands of eastern Canada, *Hydrol. Processes*, *22*, 4163–4172.

Moore, R., and S. Wondzell (2005), Physical hydrology and the effects of forest harvesting in the Pacific Northwest: A review, *J. Am. Water Resour. Assoc.*, *41*(4), 763–784.

Mwale, D., T. Y. Gan, K. J. Devito, C. A. Mendoza, U. Silins, and R. Petrone (2009), Precipitation variability and its relationship to hydrologic variability in Alberta, *Hydrol. Processes*, *23*, 3040–3056.

Peck, A. J., and D. R. Williamson (1987), Effects of forest clearing on groundwater, *J. Hydrol.*, *94*(1), 47–65.

Pomeroy, J. W., D. M. Gray, and P. G. Landine (1993), The prairie blowing snow model: Characteristics, validation, operation, *J. Hydrol.*, *144*(1-4), 165–192.

Pomeroy, J. W., D. M. Gray, K. R. Shook, B. Toth, R. H. Essery, A. Pietroniro, and N. Hedstrom (1998), An evaluation of snow accumulation and ablation processes for land surface modelling, *Hydrol. Processes*, *12*, 2339–2367.

Pothier, D., M. Prévost, and I. Auger (2003), Using the shelterwood method to mitigate water table rise after forest harvesting, *For. Ecol. Manage.*, *179*(1-3), 573–583.

Redding, T. E., and K. J. Devito (2008), Lateral flow thresholds for aspen forested hillslopes on the Western Boreal Plain, Alberta, Canada, *Hydrol. Processes*, *22*, 4287–4300, doi:10.1002/hyp.7038.

Riley, J. P., E. K. Israelsen, and K. O. Eggleston (1972), Some approaches to snowmelt prediction, in *Role of Snow and Ice in Hydrology, IAHS Publ.*, *107*, 956–971.

Roy, V., J. Jeglum, and A. Plamondon (1997), Water table fluctuations following clearcutting and thinning on Wally Creek wetlands, in *Northern Forested Wetlands: Ecology and Management*, edited by C. C. Tretin, M. F. Jurgensen, and D. F. Grigal, pp. 239–251, CRC Press, Boca Raton, Fla.

Ruprecht, J. K., and N. J. Schofield (1991), Effects of partial deforestation on hydrology and salinity in high salt storage landscapes. I. Extensive block clearing, *J. Hydrol.*, *129*(1-4), 19–38.

Sass, G. Z., and I. F. Creed (2008), Characterizing hydrodynamics on boreal landscapes using archived synthetic aperture radar imagery, *Hydrol. Processes*, *22*, 1687–1699, doi:10.1002/hyp.6736.

Si, B., R. Kachanoski, F. Zhang, G. Parkin, and D. Elrick (1999), Measurement of hydraulic properties during constant flux infiltration field average, *Soil Sci. Soc. Am. J*, *63*(4), 793–799.

Singh, P. R., T. Y. Gan, and A. K. Gobena (2009), Evaluating a hierarchy of snowmelt models at a watershed in the Canadian Prairies, *J. Geophys. Res.*, *114*, D04109, doi:10.1029/2008JD010597.

Smerdon, B. D., K. J. Devito, and C. A. Mendoza (2005), Interaction of groundwater and shallow lakes on outwash sediments in the sub-humid Boreal Plains of Canada, *J. Hydrol.*, *314*, 246–262.

Smerdon, B. D., C. A. Mendoza, and K. J. Devito (2007), Simulations of fully coupled lake-groundwater exchange in a subhumid climate with an integrated hydrologic model, *Water Resour. Res.*, *43*, W01416, doi:10.1029/2006WR005137.

Smerdon, B. D., C. A. Mendoza, and K. J. Devito (2008), The influence of subhumid climate and water table depth on groundwater recharge in shallow outwash deposits, *Water Resour. Res.*, *44*, W08427, doi:10.1029/2007WR005950.

Stagnitti, F., J. Y. Parlange, and C. Rose (1989), Hydrology of a small wet catchment, *Hydrol. Processes*, *3*, 137–150.

Stephens, D. B. (1993), A perspective on diffuse natural recharge mechanisms in areas of low precipitation, *Soil Sci. Am. J.*, *58*, 40–48.

Swanson, R. H., and R. L. Rothwell (2001), Hydrologic recovery of aspen clearcuts in northwestern Alberta, in *Sustaining Aspen in Western Landscapes: Symposium Proceedings*, edited by W. D. Shepperd et al., pp. 121–135, U.S. Dep. of Agric., Washington, D. C.

Therrien, R., R. G. McLaren, E. A. Sudicky, and S. M. Panday (2010), HydroGeoSphere: A three dimensional numerical model describing fully-integrated subsurface and surface flow and solute transport, report, Groundwater Simul. Group, Univ. of Waterloo, Waterloo, Ontario, Canada.

van Genuchten, M. T. (1980), A closed-form equation for predicting the hydraulic conductivity of unsaturated soils, *Soil Sci. Soc. Am. J*, *44*(5), 892–898.

Verry, E. S. (1987), The effect of aspen harvest and growth on water yield in Minnesota, in *Forest Hydrology and Watershed Management*, edited by R. H. Swanson, P. Y. Bernier, and P. D. Woodard, *IAHS Publ.*, *167*, 553–562.

Verseghy, D. L. (1991), CLASS: A Canadian Land Surface Scheme for GCMs. I. Soil model, *Int. J. Clim.*, *11*, 111–133.

Whitson, I., D. Chanasyk, and E. Prepas (2005), Effect of forest harvest on soil temperature and water storage and movement patterns on boreal plain hillslopes, *J. Environ. Eng. Sci.*, *4*(6), 429–439.

J. J. Carrera-Hernández, Instituto Potosino de Investigación Científica y Tecnológica, Camino a la Presa San José 2055, San Luis Potosí 78216, México. (jaime.carrera@ipicyt.edu.mx)

K. J. Devito, Department of Biological Sciences, University of Alberta, Edmonton, AB T6G 2E3, Canada.

C. A. Mendoza, Department of Earth and Atmospheric Sciences, University of Alberta, Edmonton, AB T6G 2E3, Canada.

R. M. Petrone, Department of Geography and Environmental Studies,-Wilfrid Laurier University, Waterloo, ON N2L 3C5, Canada.

B. D. Smerdon, CSIRO Land and Water, Waite Campus, Private Mail Bag 2, Glen Osmond, SA 5064, Australia.